Mass spectrometry–based proteome profile may be useful to differentiate adenoid cystic carcinoma from polymorphous adenocarcinoma of salivary glands

Felipe Paiva Fonseca, DDS, PhD,[a,b] Carolina Carneiro Soares Macedo, DDS, PhD,[a] Sara Ferreira dos Santos Costa, DDS, MSc,[b] Adriana Franco Paes Leme, DDS, PhD,[c] Romênia Ramos Rodrigues, MSc,[c] Hélder Antônio Rebelo Pontes, DDS, PhD,[d] Albina Altemani, MD, PhD,[e] Willie F.P. van Heerden, DDS, PhD, FCPath(SA)Oral,[f] Manoela Domingues Martins, DDS, PhD,[a,g] Oslei Paes de Almeida, DDS, PhD,[a] Alan Roger Santos-Silva, DDS, PhD,[a] Márcio Ajudarte Lopes, DDS, PhD,[a] and Pablo Agustin Vargas, DDS, PhD, FRCPath[a,f]

Objective. The aim of this study was to determine the proteome of adenoid cystic carcinoma (AdCC) and polymorphous adenocarcinoma (PAc) and to identify a protein signature useful in distinguishing these two neoplasms.
Study Design. Ten cases of AdCC and 10 cases of PAc were microdissected for enrichment of neoplastic tissue. The samples were submitted to liquid chromatography–tandem mass spectrometry (LC-MS/MS), and the proteomics data were analyzed by using the MaxQuant software. LC-MS/MS spectra were searched against the Human UniProt database, and statistical analyses were performed with Perseus software. Bioinformatic analyses were performed by using discovery-based proteomic data on both tumors.
Results. LC-MS/MS analysis identified 1957 proteins. The tumors shared 1590 proteins, and 261 were exclusively identified in AdCC and 106 in PAc. Clustering analysis of the statistically significant proteins clearly separated AdCC from PAc. Protein expression 10 times higher in one group than in the other led to a signature of 16 proteins—6 upregulated in AdCC and 10 in PAc. A new clustering analysis showed reverse regulation and also differentiated both tumors.
Conclusions. Global proteomics may be useful in discriminating these two malignant salivary neoplasms that frequently show clinical and microscopic overlaps, but additional validation studies are still necessary to determine the diagnostic potential of the protein signature obtained. (Oral Surg Oral Med Oral Pathol Oral Radiol 2019;128:639–650)

Salivary gland tumors (SGTs) constitute a heterogeneous group of neoplasms with complex clinical behaviors and microscopic presentations, and account for approximately 5% of all neoplasms diagnosed in the head and neck region.[1] Adenoid cystic carcinoma (AdCC) is one of the most common salivary gland malignancies, predominantly affecting the parotid gland and the minor salivary glands.[2] It is considered a high-grade neoplasm, given its significant association with late recurrences and distant metastases, leading to an unsatisfactory long-term survival.[2,3] Recently, Persson et al.[4] demonstrated that chromosomal translocation t(6;9)(q22-23;p23-24) resulting in a fusion of genes encoding the transcription factors *MYB* [v-myb myeloblastosis viral oncogene homolog (avian)] and *NFIB* (nuclear factor IB) would represent a specific molecular event in the context of SGTs, being associated with AdCC development.

Although t(6;9)(q22-23;p23-24) may not represent a prognostic determinant for AdCC,[5] the presence of this translocation contributes to distinguishing AdCC from its main differential diagnoses, which frequently represents a difficult approach, given the well-known clinical and microscopic overlaps of salivary gland neoplasms. However, in a high number of AdCC cases, t(6;9)(q22-23;p23-24) is absent, and, thus, identification of molecular markers that could better aid in the diagnosis of AdCC is warranted.[6]

Statement of Clinical Relevance

The identification of a protein signature through mass spectrometry–based proteomics may contribute to differentiating adenoid cystic carcinoma from polymorphous adenocarcinoma of salivary glands, which may represent a difficult approach, especially when dealing with small samples.

[a]Department of Oral Diagnosis, Oral Pathology Division, Piracicaba Dental School, University of Campinas (UNICAMP), Piracicaba, Brazil.
[b]Department of Surgery and Pathology, School of Dentistry, Universidade Federal de Minas Gerais, Belo Horizonte, Brazil.
[c]Laboratório de Espectrometria de Massas, Laboratório Nacional de Biociências (LNBio), Centro Nacional de Pesquisa em Energia e Materiais (CNPEM), Campinas, Brazil.
[d]Service of Oral Pathology, João de Barros Barreto University Hospital, Federal University of Pará, Belém, Brazil.
[e]Department of Pathology, School of Medical Sciences, University of Campinas (UNICAMP), Campinas, Brazil.
[f]Department of Oral Pathology and Oral Biology, School of Dentistry, University of Pretoria, Pretoria, South Africa.
[g]Department of Pathology, School of Dentistry, Federal University of Rio Grande do Sul, Porto Alegre, Brazil.
Received for publication Jan 18, 2019; returned for revision Jun 12, 2019; accepted for publication Jul 24, 2019.

2212-4403/$-see front matter
https://doi.org/10.1016/j.oooo.2019.07.016

Polymorphous adenocarcinoma (PAc) used to be considered part of the spectrum of AdCC until 1983, when PAc was first recognized as an independent entity, representing, however, one of the main mimickers of AdCC thereafter.[7] PAc is virtually restricted to the intraoral minor salivary glands, especially from the palate, where it usually presents as a slow-growing, non-aggressive tumor.[8] Molecular alterations have also been described for PAc, including mutation in the *PRKD-1* gene.[9] However, its frequency, specificity, and clinical importance must be addressed.

The search for new molecular markers that could aid in the differential diagnosis of these salivary neoplasms is still necessary, especially when only small specimens from incisional biopsies are available, a common scenario in histopathology practice. Recently, different groups have used proteomics to discover new prognostic and diagnostic markers for several human neoplastic and nonneoplastic diseases.[10,11] Mass spectrometry−based proteomics is an approach that provides large-scale data on the protein profile of tumor cells, tissues, and body fluids, and it has already been employed to detect the proteome of melanomas, head and neck, pancreatic, lung, breast, colon, and other cancers, assisting in the discovery of unknown biomarkers to improve their early detection and to better understand their pathogenesis.[11-16] Moreover, research groups have also used proteomics to obtain protein signatures or isolated proteins with potential to distinguish different neoplasms.[14,17-19] However, the proteome of SGTs is largely unknown, and the general protein expressions of AdCC and PAc remain to be determined.

Therefore, to investigate the hypothesis that AdCC and PAc could be differentiated on the basis of their proteome profiles, the objective of the present study was to identify a protein signature that could be useful in distinguishing these 2 neoplasms.

MATERIALS AND METHODS

Sample collection

This study was approved by the ethics committee of the Universidade Federal de Minas Gerais (process number CAAE 65798717.3.0000.5149). We used a convenience sample consisting of formalin-fixed, paraffin-embedded (FFPE) tissues of 10 cases diagnosed as AdCC and 10 cases diagnosed as PAc retrieved from the pathology files of the Piracicaba Dental School, University of Campinas (Piracicaba-Brazil), and the João de Barros Barreto University Hospital, Federal University of Pará (Belém-Brazil). Two authors jointly confirmed the original diagnoses by using new hematoxylin and eosin (H&E)−stained slides, according to the current World Health Organization guidelines[20] for the classification of SGTs. Clinical data regarding patient gender and age, tumor location, and symptomatology were retrieved from patients' medical charts.

Immunohistochemistry

Immunohistochemical reactions against low-molecular-weight cytokeratin (CK7), high-molecular-weight cytokeratin (CK14), S100, p63, and α-smooth muscle actin (α-SMA), which allowed for the identification of luminal and myoepithelial components, were used to better characterize the cases used. Briefly, the reactions were done in 3-μm sections of the original FFPE tissues that were dewaxed with xylene and then hydrated in a descending ethanol series. Antigen retrieval was done, and the endogenous peroxidase activity was blocked by using 10% hydrogen peroxide in 5 baths, each for 5 minutes. After washing in phosphate-buffered saline (pH 7.4), the slides were incubated overnight with primary antibodies antihuman CK7 (clone OV-TL 12/30, dilution 1:200; Leica Biosystems, Wetzlar, Germany), antihuman CK14 (clone LL002, dilution 1:200; Leica Biosystems, Wetzlar, Germany), antihuman-S100 (polyclonal, dilution 1:100; Dako, Glostrup, Denmark), antihuman p63 (clone 4 A4, dilution 1:100; Abcam, Burlingame, CA) and antihuman α-SMA (clone 1 A4, dilution 1:200; Dako, Glostrup, Denmark;). All slides were subsequently exposed to avidin−biotin complex and horseradish peroxidase reagents (LSAB Kit; Dako-Cytomation, Glostrup, Denmark) and diaminobenzidine tetrahydrochloride (DAB; Sigma, St. Louis, MO), and subsequently counterstained with Carazzi hematoxylin. Sections of lung carcinoma, normal skin, normal nerve, fibrous hyperplasia with overlying surface epithelium, and endometrium were used as positive controls for each antibody, respectively. The negative control was obtained by omitting the primary specific antibody. Results were evaluated by one oral pathologist.

Sample preparation and laser microdissection

A new histologic slide was prepared for each of the 20 SGTs investigated. Paraffin blocks were cut by microtome with a thickness of 5 μm and another slide with 10 μm of thickness. Histologic section of 5 μm was stained with H&E to guide laser microdissection (LMD). The other section (10 μm) was prepared by using specific membrane slides for LMD (PEN Arcturus Membrane; Life Technologies, Carlsbad, CA), stained with hematoxylin, submitted to dehydration in ethanol 90% and 100%, and stored in containers before drying and LMD.

Samples were processed by using Leica Laser Microdissection Systems (Leica Biosystems, Wetzlar, Germany). Only neoplastic cells were microdissected and collected. An average of 6.000.000μm^2 of each tissue was obtained.

All samples were collected in 600-μL microtubes and stored at −80°C. LMD was standardized for FFPE tissues with a slice depth of 10 μm. The adjustable parameters in LMD Laser Microdissection Leica software (Leica Biosystems, Wetzlar, Germany) are considered optimal for these samples, and the area (μm^2) cut for each patient was recorded.

Protein extraction and trypsin digestion

Protein extraction and digestion were performed according to the protocol developed previously.[21-24] Samples were treated with 8 M urea, followed by protein reduction with dithiothreitol (5 mM for 25 minutes at 56°C) and alkylation with iodoacetamide (14 mM for 30 minutes at room temperature in the dark). For protein digestion, urea was diluted to a final concentration of 1.6 M, and 1 mM of calcium chloride was added to the samples for trypsin digestion for 16 hours at 37°C (2 μg of trypsin). The reaction was quenched with 0.4% formic acid, and peptides were desalted by stage tips C18.[25]

Liquid chromatography−tandem mass spectrometry analysis

An aliquot containing 4.5 μL of peptide mixture was analyzed on an LTQ Orbitrap Velos (ThermoFisher Scientific, Waltham, MA) mass spectrometer coupled to nanoflow liquid chromatography on the EASY-nLC system (Proxeon Biosystems, Odense, Denmark) through a Proxeon nanoelectrospray ion source. Peptides in 0.1% formic acid were separated by a 2% to 90% acetonitrile gradient in a PicoFrit analytical column (20 cm × ID75, 5-μm particle size, New Objective), with a flow rate of 300 nL/min over 212 minutes, as previously described.[12]

Proteomics data analysis

The raw files were processed by using the MaxQuant (Prof. Cox J, Max-Planck-Gesellschaft, München, Germany) v1.3.0.3 software,[24] and MS/MS spectra were searched against the Human UniProt database (released May 2017; 92,646 sequences; 36,874,315 residues) by using the Andromeda search engine.[26] A tolerance of 6 ppm was considered for precursor ions and 0.5 Da for fragment ions. Oxidation of methionine and protein N-terminal acetylation was set as variable modifications and carbamidomethylation of cysteine as fixed modification and with 2 missed trypsin cleavage. Label-free quantification (LFQ) was used for protein quantification, with a 2-minute window for matching between runs and minimal ratio count set as 1. The false discovery rate for protein and peptide was set at 1%. Statistical analysis was performed with Perseus (Prof. Cox J, Max-Planck-Gesellschaft, München, Germany) v1.2.7.4 software.[24] Protein data set were processed after excluding reverse sequences and "only identified by site" entries, and then the data were transformed by log2. In addition, it was considered in the final analysis of a minimum of 3 valid values in at least one group, and statistical significance was assessed by Student *t* test to indicate the differentially expressed proteins ($P < .05$).

Additionally, the files containing the identified proteins and their LFQ intensity values were used for clustering and heat map generation. Heat maps, hierarchical clustering, and principal component (PC) analysis were constructed in the Web-based chemometrics platform MetaboAnalyst (Xia Lab, McGill University, Montreal, Canada) 3.0 by using the Pearson distance measure.

Bioinformatics analysis

Proteins with differential expression between the AdCC and PAc groups were submitted to an enrichment analysis to gain biologic information from this list of the identified proteins. Uniprot IDs of differential proteins were submitted to the Integrated Interactome System (Carazzolle MF et al. Brazilian Center for Research and Materials; Laboratório Nacional de Biociência, Campinas Brazil) platform[27] to perform the enrichment analysis for the GO (Gene Ontology)[28] database. Only significant biologic processes (P value $< .05$) were considered in the results. Protein−protein association networks were constructed in the STRING database.[29]

RESULTS

Clinicopathologic data from patients

The clinicopathologic features of the 20 cases investigated in this study are detailed in Table I. Briefly, females predominated in both groups (7:3 in the AdCC group and 6:4 in the PAc group); mean age was 48.2 years and 54.4 years in the AdCC and PAc groups, respectively. The palate was the sites most affected by both tumors and a painful symptomatology was present in 5 patients affected by AdCC and in 3 affected by PAc (Figure 1). Microscopically, AdCC cases demonstrated a predominance of the cribriform architectural pattern characterized by pseudocystic spaces filled with homogeneous hyaline substance and surrounded by neoplastic cells exhibiting scarce cytoplasm and hyperchromatic nuclei. Bilayered ductal structures were also present. PAc predominantly had a lobular architectural pattern, with the so-called targetoid growth pattern present in 3 of the cases. Single line arrangement of neoplastic cells was also found. Tumor cells were round, with pale stained nuclei (Figure 2). Immunohistochemistry was performed to better characterize the cellular components of both

Table I. Clinical data of the 20 cases included in the study

No.	*Diagnosis*	*Gender*	*Age*	*Site*	*Symptomatology*
1	AdCC	M	46	Minor gland – Palate	Painless
2	AdCC	F	41	Minor gland – lip	Painful
3	AdCC	F	58	Minor gland – floor of the mouth	Painless
4	AdCC	F	69	Minor gland – palate	Painless
5	AdCC	M	34	Minor gland – buccal mucosa	Painful
6	AdCC	F	76	Parotid gland	Painful
7	AdCC	M	52	Minor gland – palate	Painful
8	AdCC	F	39	Minor gland – palate	Painful
9	AdCC	F	37	Submandibular gland	Painless
10	AdCC	F	30	Minor gland – palate	Painless
11	PAc	M	70	Minor gland – palate	Painless
12	PAc	F	51	Minor gland – palate	Painful
13	PAc	F	48	Minor gland – palate	Painless
14	PAc	F	48	Minor gland – palate	Painful
15	PAc	M	80	Minor gland – upper lip	Painless
16	PAc	F	64	Minor gland – buccal mucosa	Painless
17	PAc	F	40	Minor gland – palate	Painless
18	PAc	M	45	Minor gland – palate	Painless
19	PAc	F	60	Minor gland – palate	Painful
20	PAc	M	38	Minor gland – upper lip	Painless

AdCC, adenoid cystic carcinoma; *F,* female; *M,* male; *PAc,* polymorphous adenocarcinoma.

tumors. AdCC exhibited strong positivity for CK7 (in the luminal cells of the ductal structures) and for CK14 (myoepithelial cells), as well as a strong positivity for p63 and α-SMA in the myoepithelial cells. S100 was positive only in myoepithelial cells. PAc was strongly and diffusely positive for CK7 and S100, with focal positivity to p63 and CK14, and negativity for α-SMA (Figure 3).

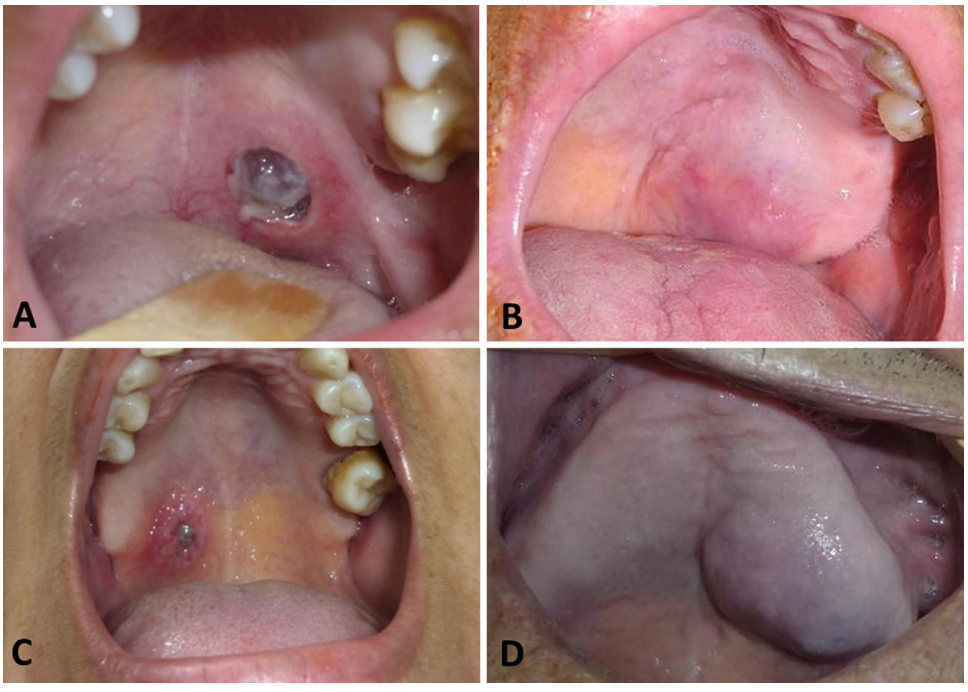

Fig. 1. Representative images of adenoid cystic carcinoma (AdCC) and polymorphous adenocarcinoma (PAc) demonstrating the important overlap observed in the clinical presentation of these malignant neoplasms. **A,** AdCC may clinically present as a painful, ulcerative lesion in the palate. **B,** However, it is more commonly diagnosed as an asymptomatic, slow-growing swelling affecting the minor glands of the palate. **C,** PAc may also show an ulcer. **D,** Or it may present as a slow-growing painless tumor in the oral cavity.

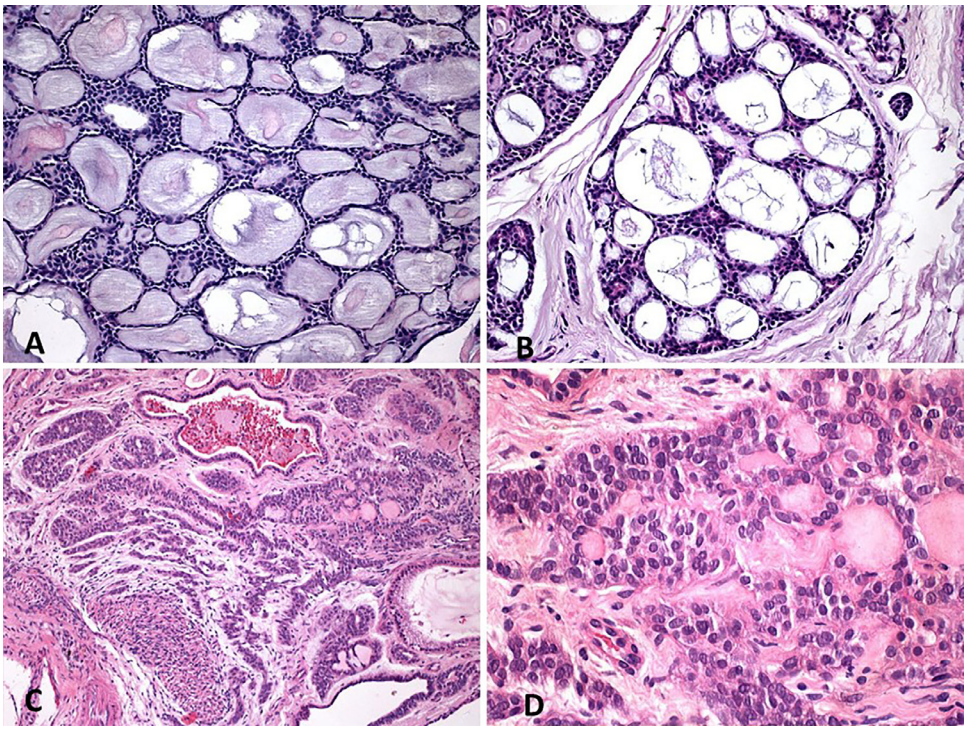

Fig. 2. Microscopic aspect of the adenoid cystic carcinoma (AdCC) and polymorphous adenocarcinoma (PAc) cases used in this study. **A,** Characteristic cribriform growth pattern of AdCC (hematoxylin and eosin [H&E]; magnification × 100). **B,** In the cribriform structures of AdCC, it was possible to observe more eosinophilic luminal epithelial cells forming small ductal structures (H&E; 100 X). C) PAc case containing neoplastic cells that exhibited foci of neural involvement (H&E; magnification × 100). **D,** Under higher magnification, it is possible to observe the pale staining and the blended appearance of PAc cells (H&E; magnification × 200).

Association of LMD and LC-MS/MS is able to identify the proteome of AdCC and PAc

The LMD approach enabled individualization of the tumor regions from AdCC and PAc, thus separating the neoplastic cells from adjacent normal tissue.

LC-MS/MS analysis identified a total of 1957 proteins (Supplementary Tables 1 to 3). In a Venn diagram, it is possible to verify the number of proteins shared between AdCC and PAc, as well as the proteins found exclusively in each tumor (Figure 4A). A total of 1590 proteins were shared between the tumors studied, with 261 proteins identified only in the AdCC cases (Supplementary Table 4) and 106 proteins only in PAc (Supplementary Table 5).

LC-MS/MS analysis revealed abundant differentially expressed proteins in AdCC and PAc

LC-MS/MS analysis revealed differentially expressed proteins in AdCC and PAc. Student *t* test analyses performed with the Perseus software identified differentially expressed proteins ($P \leq .05$) in these two malignant SGTs.

Of the 1957 proteins identified in total, 394 proteins showed a statistically significant difference in their expression in AdCC and PAc (Supplementary Table 6). Clustering analyses, first using all proteins identified and then using statistically significant proteins, showed a clear separation of the tumors, with distinct protein expression patterns (Figures 4B and 4C). Moreover, PC analysis was performed to transform and cluster AdCC and PAc global data sets in an unsupervised fashion. PC 1 and PC 2 presented 16.4% and 10.3% of variance, respectively, demonstrating a clear data segregation. Therefore, PC analysis confirmed the distinct proteomes exhibited by AdCC and PAc (Figure 4D).

Proteins with statistically significant differences in expression were then correlated with biologic processes in an enriched analysis. Thus, 243 proteins showed a statistically significant association with 80 biologic processes ($P \leq .05$) (Supplementary Table 7). The top 10 enriched biologic processes were associated with proteins that play a role in tumor progression, such as small molecule metabolic process, extracellular matrix organization, extracellular matrix disassembly, messenger RNA (mRNA) splicing via spliceosome, RNA splicing, osteoblast differentiation, immune response, cell adhesion, and gene expression (Figure 5).

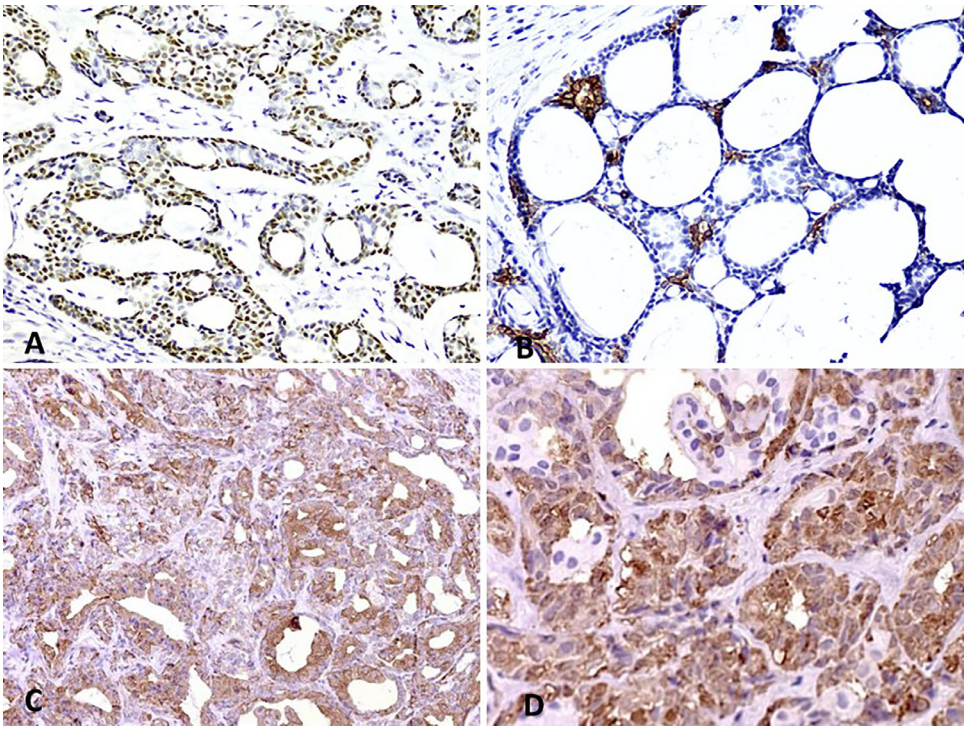

Fig. 3. Immunohistochemical reactions used to better characterize the cellular components of adenoid cystic carcinoma (AdCC) and polymorphous adenocarcinoma (PAc) cases. **A,** p63 strong nuclear positivity in the myoepithelial cells of AdCC (3,3′-diaminobenzidine [DAB]; magnification × 200). **B,** CK7 stained the luminal cells of small ductal structures observed in AdCC cases (DAB; magnification × 200). **C,** In PAc, CK7 revealed a more diffuse positive staining (DAB; magnification × 200). **D,** Similarly, PAc cases also demonstrated a strong and diffuse positivity for S100 (DAB; magnification × 200).

Proteome annotation indicated signature proteins and distinct protein expression to differentiate AdCC from PAc

We combined the data from the Student *t* test and the enriched biologic process with the expression of proteins in each tumor. On the basis of previous publications, a fold-change higher than 10 times in one group than in the other was considered the cutoff value to decrease the number of candidate proteins and to create a protein signature with a higher potential of diagnostic determination.[30-32] Through this combination of data, we arrived at a signature of 16 proteins, 6 upregulated in AdCC and 10 in PAc (Table II). To confirm the significant differences in the expressions of these 16 proteins in both tumors, a new clustering analysis was done, showing separation of the groups and a trend toward a reverse regulation, for instance, COL7A1 was upregulated in AdCC and downregulated in PAc. This cluster analysis with the 16 signature proteins revealed clear differences between AdCC and PAc (Figure 6).

DISCUSSION

Diagnosis of SGTs, given their highly heterogeneous microscopic aspects and similar clinical manifestations, frequently represents a challenge even for experienced diagnosticians. Moreover, the lack of reliable diagnostic markers also contributes to difficulty in the recognition of these tumors. Therefore, the use of strategies that would lead to the discovery of new molecules that could contribute to improving the diagnosis of these neoplasms is mandatory. In this study, we performed a comparative proteome analysis to examine the global differences in the protein expression patterns of AdCC and PAc, and our results demonstrated that the mass spectrometry approach was useful to obtain a proteomic signature that significantly differentiated both tumors.

AdCC and PAc are two frequently encountered malignant SGTs that demonstrate clinical and microscopic overlaps.[7] These neoplasms usually manifest as slow-growing swellings that more commonly affect the parotid glands and the minor salivary glands of the oral cavity, respectively.[8,33] Pain may be reported, whereas ulcers are only occasionally observed. Microscopically, in both tumors, neural invasion and a cribriform growth pattern are common findings.[33,34] Although some histologic features and the use of some nonspecific immunohistochemical markers may contribute to differentiating between these malignancies, this may be exceedingly difficult in some cases, especially in those with limited tissue availability; this is an important issue, given the poor prognosis carried by AdCC, frequently associated with late recurrences and distant metastases.[8,33,35]

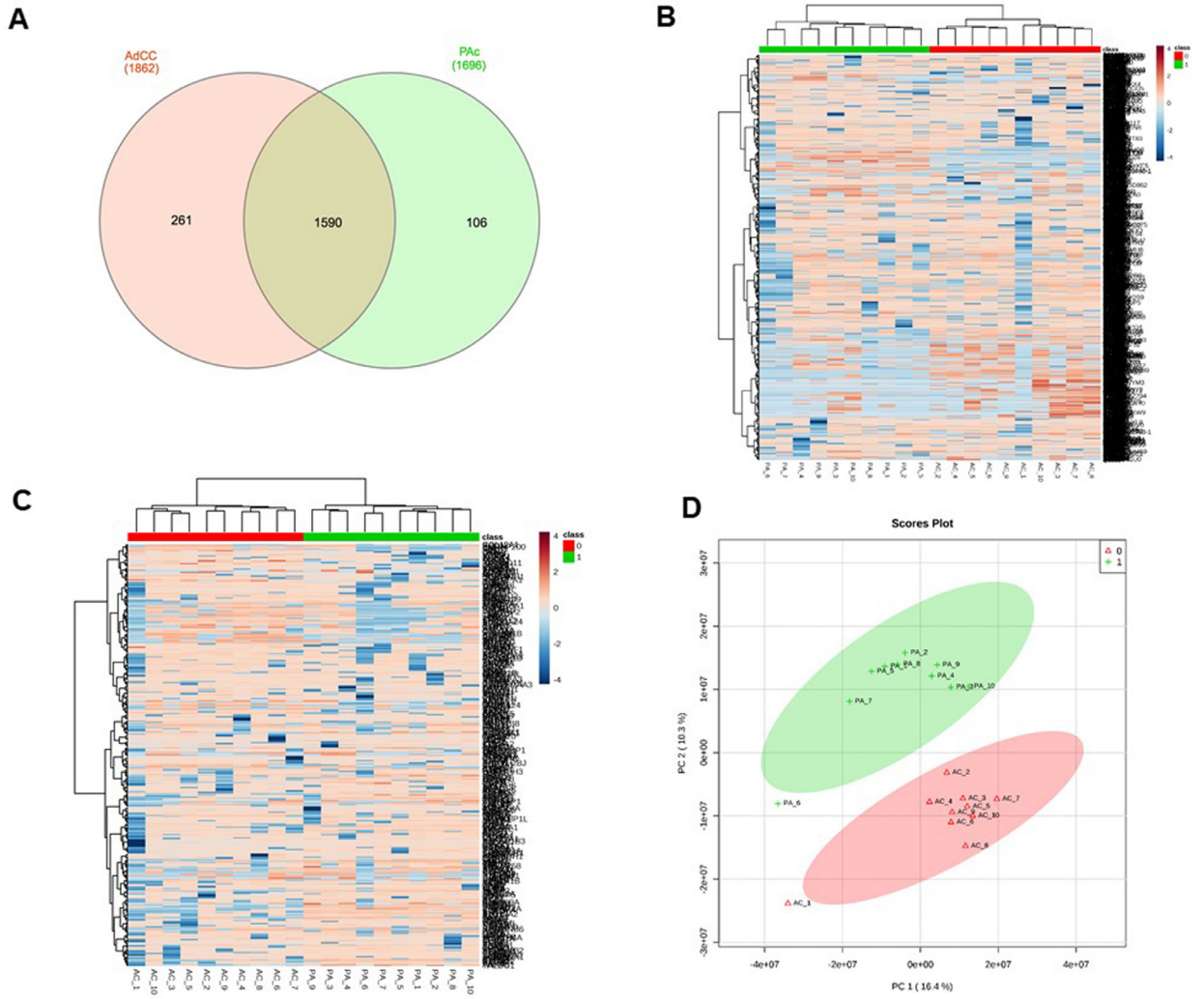

Fig. 4. Quantitative proteome analysis differentiates adenoid cystic carcinoma from polymorphous adenocarcinoma (PAc). **A,** Venn diagram of common and exclusive proteins identified for adenoid cystic carcinoma (AdCC) and PAc. **B,** Analysis of clustering of the 1957 proteins identified in both tumors. The values for each protein *(lines)* and for each microdissected sample *(columns)* are colored based on the abundance of protein, in which high *(red)* and low *(blue)* values (using the Z-score LFQ values) are indicated in the scale color bar at the bottom. The hierarchical grouping was performed in the MetaboAnalyst 3.0 software using Pearson's correlation for data. **C,** Heat map of the differentially expressed proteins between AdCC and PAc. Proteins identified in tumors were hierarchically clustered by using the Z-score label-free quantification (LFQ) values with MetaboAnalyst 3.0 software. This cluster analysis revealed significant differences between AdCC and PAc. **D,** Score-plot of the PC analysis performed also in Metaboanalyst 3.0 showed the variance in the data among the two components that were derived from this analysis, with clear separation. PC 1 presented 16.4% of the variance, and PC 2 presented 10.3% of the variance.

Although recent studies have demonstrated that these tumors are characterized by the presence of different and specific genetic events, such as the translocation involving the genes *MYB* and *NFIB* on chromosomes 6 and 9 in AdCC and mutations in the *PRKD1* gene in PAc, these molecular imbalances are not always present, and the needed access to specialized laboratories to identify these mutations for routine microscopic diagnosis is still limited.[6] Different groups have identified the use of proteomics to find new molecular markers with not only diagnostic potential but also prognostic potential, as well as those involved in the pathogenesis of different cancerous and noncancerous diseases that could later be identified by more accessible laboratory techniques, such as immunohistochemistry.[36,37]

Using mass spectrometry, Flores et al.[38] identified 388 proteins exclusively expressed in oral squamous cell carcinoma compared with those expressed in the normal oral mucosa, subsequently demonstrating that one of these proteins, EEF1D, would play an important role in the pathogenesis of this aggressive cancer. Similarly, Kawahara et al.[10] used targeted proteomics to

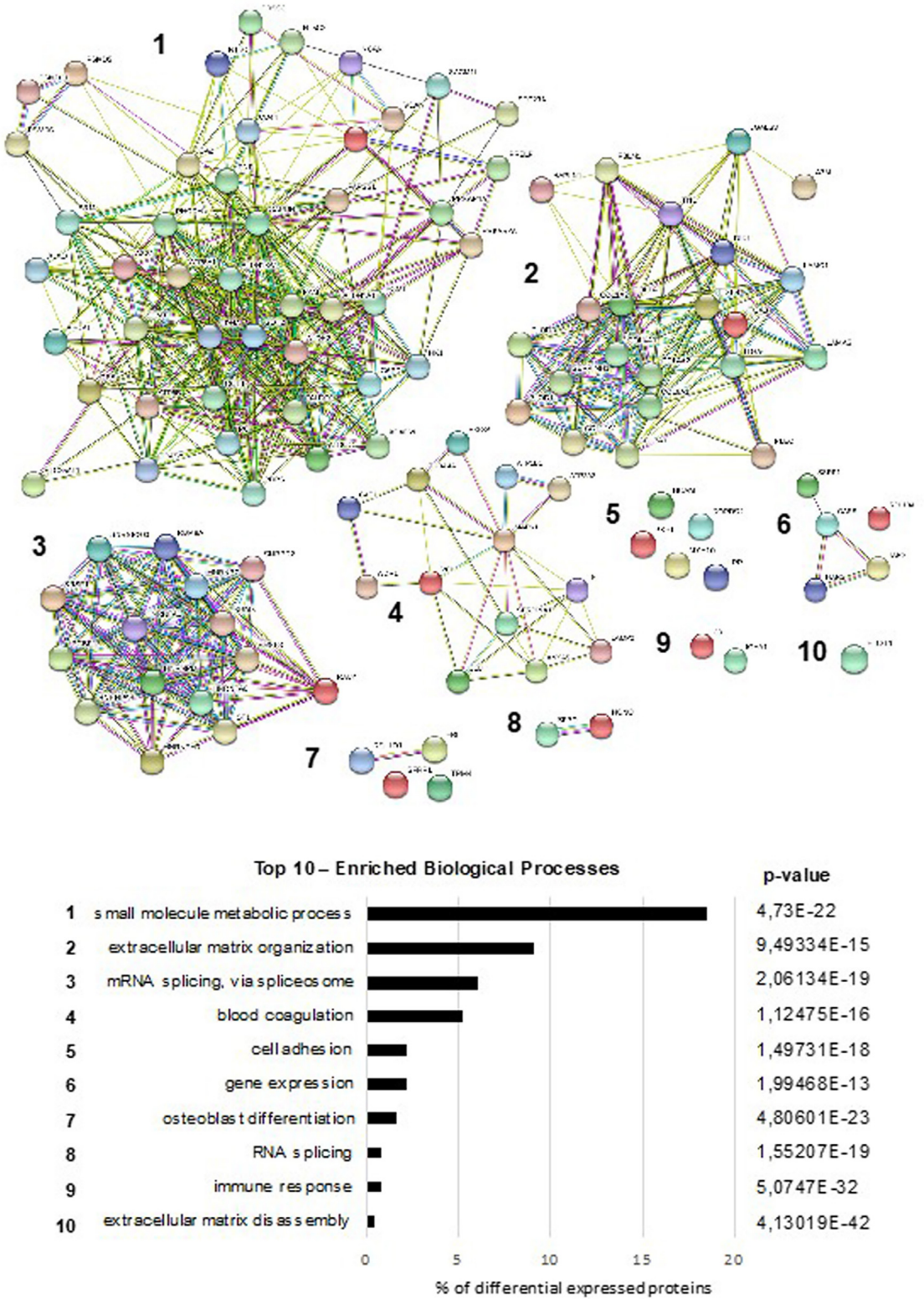

Fig. 5. Top 10 enriched biologic processes. The enrichment analysis for the GO (Gene Ontology) database identified 80 significant biologic processes in adenoid cystic carcinoma (AdCC) and polymorphous adenocarcinoma (PAc), involving 243 differentially expressed proteins (see Supplementary Table 7). A schematic representation of the top 10 enriched biologic processes shared by both tumors is showed, with protein-interaction networks constructed in the STRING database.

Table II. Upregulated and downregulated proteins identified in AdCC and PAc of salivary glands (minimum fold change of 10)

Protein ID	*UniProt ID*	*Protein name*	*Top enriched BP*	*Ratio in AdCC**	*Ratio in PAc†*	*Expression*	*P values*
COL7A1	Q02388	Collagen alpha-1(VII) chain	Extracellular matrix organization	143.9470886	.006946997	Upregulated in AdCC	.00046386
HAPLN1	P10915	Hyaluronan and proteoglycan link protein 1	Extracellular matrix organization	56.40366049	.017729346	Upregulated in AdCC	2.3543E−6
ACTA2	P62736	Actin, aortic smooth muscle	Muscle contraction	24.66728711	.040539521	Upregulated in AdCC	.02137686
TUBA1A	Q71U36	Tubulin alpha-1 A chain	Mitotic cell cycle	15.22867117	.065665611	Upregulated in AdCC	.04970298
FBLN1	P23142	Fibulin-1	Extracellular matrix organization	15.17372016	.065903417	Upregulated in AdCC	.00180606
PKP1	Q13835	Plakophilin-1	Cell adhesion	12.59913473	.07937053	Upregulated in AdCC	.04949547
NCAN	O14594	Neurocan core protein	Small molecule metabolic process	.010056395	99.43921476	Upregulated in PAc	.00268849
ALDH1A1	P00352	Retinal dehydrogenase 1	Small molecule metabolic process	.016975038	58.9100287	Upregulated in PAc	1.7472 E-07
S100A1	Q5T7Y6	Protein S100-A1	Regulation of heart contraction	.029050413	34.42291807	Upregulated in PAc	.04659331
SLC12A2	P55011	Solute carrier family 12 member 2	Transmembrane transport	.031889967	31.35782518	Upregulated in PAc	8.4007E−7
PRKAR1A	P10644	cAMP-dependent protein kinase type I-alpha regulatory subunit	Small molecule metabolic process	.057774688	17.30861806	Upregulated in PAc	2.9863E−7
ATP1B1	P05026	Sodium/potassium-transporting ATPase subunit beta-1	Blood coagulation	.062138003	16.09321107	Upregulated in PAc	.01256684
TNC	P24821	Tenascin	Extracellular matrix organization	.063413384	15.76954162	Upregulated in PAc	4.0042E−7
COPS7A	Q9UBW8	COP9 signalosome complex subunit 7 a	Cullin deneddylation	.069808625	14.3248,7744	Upregulated in PAc	6.2297E−5
SYNM	O15061	Synemin	Intermediate filament cytoskeleton organization	.072650241	13.76457924	Upregulated in PAc	9.4936E−7
NDRG1	Q92597	NDRG1	Cell death	.086140994	11.60887469	Upregulated in PAc	4.3605E−6

Values represent the fold of expression in AdCC in relation to PAc and in polymorphous adenocarcinoma in relation to AdCC.

*Upregulated in AdCC and downregulated in PAc.

†Upregulated in PAc and downregulated in AdCC.

AdCC, adenoid cystic carcinoma. *BP,* biologic processes; *PAc,* polymorphous adenocarcinoma.

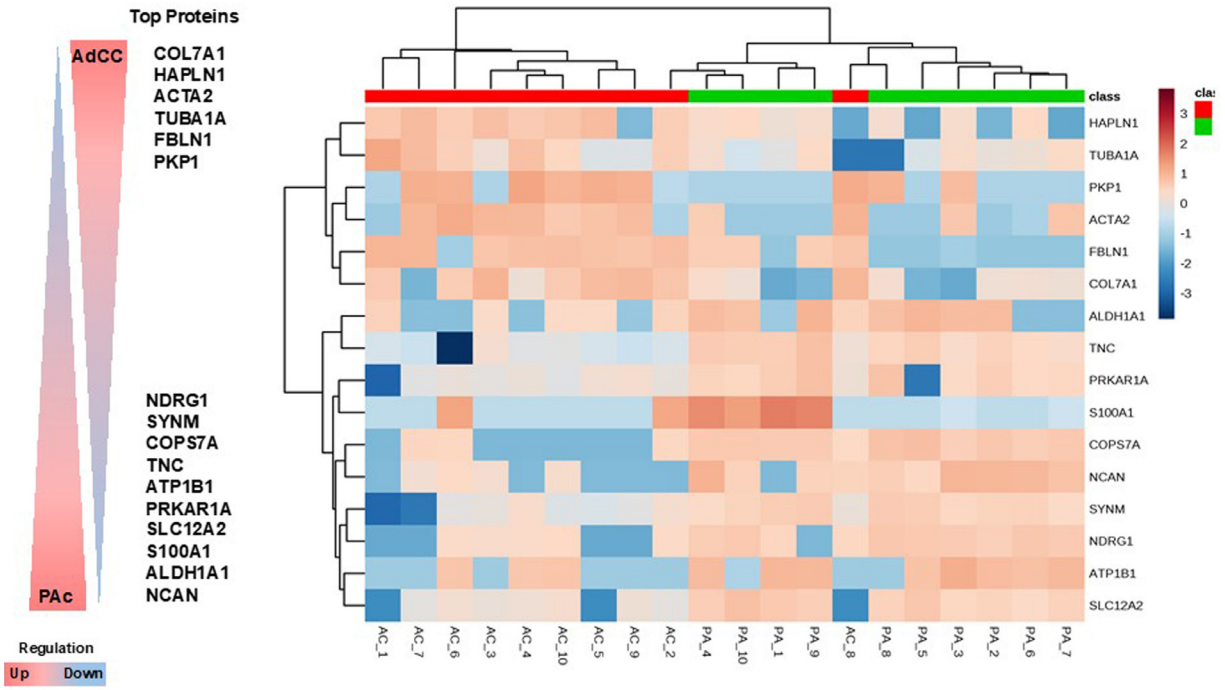

Fig. 6. Reverse regulation of the signature proteins differentially expressed between adenoid cystic carcinoma (AdCC) and polymorphous adenocarcinoma (PAc). Heat map of the 16 top differentially expressed proteins between AdCC and PAc. Signature proteins identified in tumors were hierarchically clustered by using label-free quantification (LFQ) values with MetaboAnalyst 3.0 software. This cluster analysis revealed a reverse regulation of the proteins, likewise represented in the schematic figure: Although COL7A1, HAPLN1, ACTA2, TUBA1A, FBLN1 and PKP1 were upregulated in AdCC, they were also downregulated in PAc. In the same way, although NCAN, ALDH1A1, S100A1, SLC12A2, PRKAR1A, ATP1B1, TNC, COPS7 A, SYNM and NDRG1 were upregulated in PAc, they were also downregulated in AdCC.

measure in saliva a panel of biomarker candidates for increased risk of oral squamous cell carcinoma and observed that CFB, C3, C4B, SERPINA1, and LRG1 were associated with a higher risk of this malignancy. Johnston et al.,[37] using normal B lymphocytes, recently showed the ability of proteomics to identify previously unknown potential molecular targets for chronic lymphocytic leukemia, as well as a protein expression signature for this neoplasm. These results are in agreement with those of Giusti et al.,[17] who using fine-needle aspiration fluids, found 17 differentially expressed proteins between two variants of papillary thyroid cancers.

In the context of SGTs, Donadio et al.[18] investigated the proteomic profile of pleomorphic adenoma and Warthin tumor. Those authors demonstrated a total of 26 differentially expressed proteins, further validating 9 of them as potential diagnostic markers. To date, this was the only study investigating the proteomic profile of SGTs available in literature. There seems to be no previous attempts to determine the proteomes of AdCC and PAc of salivary glands, and our results corroborate the findings of Donadio et al.,[18] demonstrating that it is possible to obtain a global protein profile that can differentiate both tumors and to obtain a protein signature of 16 molecules with a significantly different expression patterns in AdCC and PAc, indicating that the use of this combination of differentially expressed proteins could be a useful diagnostic auxiliary in those cases where routine histology is not sufficient.

Furthermore, we observed that this protein signature of 16 biomarkers demonstrated different trends toward reverse regulation in AdCC and PAc. For instance, the collagen type VII α1 chain (COL7A1) protein exhibited an expression 143 times higher in AdCC than in PAc. COL7A1 is a basement membrane protein responsible to form anchoring fibrils that may contribute to the organization and adhesion of the epithelial basement membrane, interacting with extracellular matrix proteins, and was associated with the development of esophageal squamous cell carcinoma. In a recent study, Tao et al.[39] investigated the single fused RNA sequence of COL7A1 and urocortin 2 (UCN2) in laryngeal cancer and found that this chimera COL7A1-UCN2 affected cancer stem cell transition, promoted epithelial−mesenchymal transition, and resulted in poorer prognosis.

However, NCAN (neurocan core protein) had an expression 99 times higher in PAc than in AdCC. NCAN is a chondroitin sulfate proteoglycan that modulates neuronal adhesion and has recently been associated with neuroblastoma progression. Su et al.[40]

studied the role of NCAN in neuroblastomas, observing that this protein was highly upregulated in malignant cells, promoting malignant phenotype acquisition and cell division. To date, no study has investigated COL71A and NCAN protein expressions in AdCC and PAc.

It is also important to observe that the S100A1 protein was shown to be upregulated in PAc cases compared with AdCC, which would be in agreement with the observed findings in immunohistochemical analyses and those already reported in the literature[41] because S100 positivity in AdCC is restricted to its myoepithelial component and diffusely present in PAc tumor cells. However, our proteomics results refer more specifically to the S100A1 subtype, whose distribution in AdCC and PAc remains to be investigated.

Although laser microdissection does not avoid the occasional stromal tissue included in the samples submitted to spectrometry analysis, in this study, we attempted to enrich as much of our samples as possible for neoplastic cells only; therefore, we assume that any diagnostic potential of the 16 biomarkers present in the protein signature obtained may rely on their expression in the parenchymal component of the neoplasms, not in their stromal compartment, and this deserves to be evaluated in future investigations. In addition, an important component of a high-throughput study, such as proteomics analysis, is the follow-up validation; this applies to our study also because we used a small convenience sample of 10 cases for each tumor to determine their proteomic profiles; therefore, we understand that the diagnostic potential of the proteins exclusively expressed by each tumor and those differentially expressed in the neoplasms described in our study must be validated in a larger independent sample of AdCC and PAc cases using other laboratorial methodologies, such as immunohistochemistry and Western blot analysis. However, we also believe that the preliminary results presented here may be useful to other groups in conducting their own analyses on the expression of different proteins in these two neoplasms.

CONCLUSIONS

Our study findings demonstrate that global proteomics may be useful to distinguish two malignant SGTs that frequently show very similar clinical and microscopic features, although additional validation studies are still necessary to confirm and to determine the diagnostic potential of the protein signature obtained here.

FUNDING

This study was funded by the São Paulo State Research Foundation (FAPESP), multiuser Project FAPESP 2009/54067-3; and a postdoctoral scholarship (Project FAPESP 2015/16056-0).

PRESENTATION

The present study was presented as a poster during the 44th Brazilian Meeting of Oral Pathology and Medicine (17th - 20th July 2018) in Rio de Janeiro.

ACKNOWLEDGMENTS

We acknowledge that Dr. Felipe Paiva Fonseca received a postdoctoral scholarship from the São Paulo State Research Foundation (FAPESP Process# 2015/16056-0). We also acknowledge the mass spectrometry group at Brazilian Biosciences National Laboratory (LNBio), CNPEM, Campinas, Brazil, for their support with the use of NanoLC PROXEON EASY-nLC II coupled with LTQ Orbitrap Velos ETD mass spectrometer (ThermoFisher Scientific, Waltham, MA) (Financial Support: FAPESP multi-user Project 2009/54067-3).

SUPPLEMENTARY MATERIALS

Supplementary material associated with this article can be found in the online version at doi: 10.1016/j.oooo.2019.07.016.

REFERENCES

1. Fonseca FP, Carvalho MV, de Almeida OP, et al. Clinicopathologic analysis of 493 cases of salivary gland tumors in a Southern Brazilian population. *Oral Surg Oral Med Oral Pathol Oral Radiol*. 2012;114:230-239.
2. Coca-Pelaz A, Rodrigo JP, Bradley PJ, et al. Adenoid cystic carcinoma of the head and neck—An update. *Oral Oncol*. 2015;51:652-661.
3. Agarwal JP, Jain S, Gupta T, et al. Intraoral adenoid cystic carcinoma: prognostic factors and outcome. *Oral Oncol*. 2008;44:986-993.
4. Persson M, Andrén Y, Mark J, Horlings HM, Persson F, Stenman G. Recurrent fusion of MYB and NFIB transcription factor genes in carcinomas of the breast and head and neck. *Proc Natl Acad Sci U S A*. 2009;106:18740-18744.
5. Almeida-Pinto YD, Costa SFS, Andrade BAB, et al. t(6;9) (MYB-NFIB) in head and neck adenoid cystic carcinoma: a systematic review with meta-analysis. *Oral Dis*. 2019;25:1277-1282.
6. Fonseca FP, Sena Filho M, Altemani A, Speight PM, Vargas PA. Molecular signature of salivary gland tumors: potential use as diagnostic and prognostic marker. *J Oral Pathol Med*. 2016;45:101-110.
7. Fonseca FP, Brierley D, Wright JM, et al. Polymorphous low-grade adenocarcinoma of the upper lip: 11 cases of an uncommon diagnosis. *Oral Surg Oral Med Oral Pathol Oral Radiol*. 2015;119:566-571.
8. Elhakim MT, Breinholt H, Godballe C, et al. Polymorphous low-grade adenocarcinoma: a Danish national study. *Oral Oncol*. 2016;55:6-10.
9. Weinreb I, Piscuoglio S, Martelotto LG, et al. Hotspot activating PRKD1 somatic mutations in polymorphous low-grade adenocarcinomas of the salivary glands. *Nat Genet*. 2014;46:1166-1169.
10. Kawahara R, Bollinger JG, Rivera C, et al. A targeted proteomic strategy for the measurement of oral cancer candidate biomarkers in human saliva. *Proteomics*. 2016;16:159-173.

11. Mueller C, Haymond A, Davis JB, Williams A, Espina V. Protein biomarkers for subtyping breast cancer and implications for future research. *Expert Rev Proteomics*. 2018;15:131-152.
12. Kawahara R, Meirelles GV, Heberle H, et al. Integrative analysis to select cancer candidate biomarkers to targeted validation. *Oncotarget*. 2015;6:43635-43652.
13. Rodríguez-Cerdeira C, Molares-Vila A, Carnero-Gregorio M, Corbalan-Rivas A. Recent advances in melanoma research via "omics" platforms. *J Proteomics*. 2018;188:152-166.
14. Shoshan-Barmatz V, Bishitz Y, Paul A, et al. A molecular signature of lung cancer: potential biomarkers for adenocarcinoma and squamous cell carcinoma. *Oncotarget*. 2017;8:105492-105509.
15. Park J, Lee E, Park KJ, et al. Large-scale clinical validation of biomarkers for pancreatic cancer using a mass spectrometry-based proteomics approach. *Oncotarget*. 2017;8:42761-42771.
16. Hu HF, Xu WW, Wang Y, et al. Comparative proteomics analysis identifies Cdc42-Cdc42 BPA signaling as prognostic biomarker and therapeutic target for colon cancer invasion. *J Proteome Res*. 2018;17:265-275.
17. Giusti L, Iacconi P, Ciregia F, et al. Fine-needle aspiration of thyroid nodules: proteomic analysis to identify cancer biomarkers. *J Proteome Res*. 2008;7:4079-4088.
18. Donadio E, Giusti L, Seccia V, et al. New insight into benign tumours of major salivary glands by proteomic approach. *PLoS One*. 2013;8:E71874.
19. Ciregia F, Giusti L, Molinaro A, et al. Proteomic analysis of fine-needle aspiration in differential diagnosis of thyroid nodules. *Transl Res*. 2016;176:81-94.
20. Bell D, Bullerdiek J, Gnepp DR, et al. International Agency for Research on Cancer (IARC). Salivary gland tumours. In: El-Naggar AK, Chan JKC, Grandis JR, Takata T, Slootweg PJ, eds. *World Health Organization Classification of Head and Neck Tumours*, Lyon, France: IARC Press; 2017. p. 33.
21. Ostasiewicz P, Zielinska DF, Mann M, Wisniewski JR. Proteome, phosphoproteome, and n-glycoproteome are quantitatively preserved in formalin-fixed paraffin-embedded tissue and analyzable by high-resolution mass spectrometry. *J Proteome Res*. 2010;9:3688-3700.
22. Villén J, Gygi SP. The SCX/IMAC enrichment approach for global phosphorylation analysis by mass spectrometry. *Nat Protoc*. 2008;3:1630-1638.
23. Carnielli CM, Macedo CCS, De Rossi T, et al. Combining discovery and targeted proteomics reveals a prognostic signature in oral cancer. *Nat Commun*. 2018;9:3598.
24. Cox J, Mann M. MaxQuant enables high peptide identification rates, individualized p.p.b.-range mass accuracies and proteome-wide protein quantification. *Nat Biotechnol*. 2008;26:1367-1372.
25. Rappsilber J, Mann M, Ishihama Y. Protocol for micro-purification, enrichment, pre-fractionation and storage of peptides for proteomics using StageTips. *Nat Protoc*. 2007;2:1896-1906.
26. Cox J, Neuhauser N, Michalski A, Scheltema RA, Olsen JV, Mann M. Andromeda: a peptide search engine integrated into the MaxQuant environment. *J Proteome Res*. 2011;10:1794-1805.
27. Carazzolle MF, Carvalho LM, Slepicka HH, et al. IIS-Integrated Interactome System: a web-based platform for the annotation, analysis and visualization of protein−metabolite−gene−drug interactions by integrating a variety of data sources and tools. *PLoS One*. 2014;9:E100385.
28. Ashburner M, Ball CA, Blake JA, et al. Gene ontology: tool for the unification of biology. The Gene Ontology Consortium. *Nat Genet*. 2000;25:25-29.
29. Szklarczyk D, Morris JH, Cook H, et al. The STRING database in 2017: quality-controlled protein-protein association networks, made broadly accessible. *Nucleic Acids Res*. 2017;45:D362-D368.
30. Molloy MP, Donohoe S, Brzezinski EE, et al. Large-scale evaluation of quantitative reproducibility and proteome coverage using acid cleavable isotope coded affinity tag mass spectrometry for proteomic profiling. *Proteomics*. 2005;5:1204-1208.
31. Gygi SP, Rist B, Griffin TJ, Eng J, Aebersold R. Proteome analysis of low-abundance proteins using multidimensional chromatography and isotope-coded affinity tags. *J Proteome Res*. 2002;1:47-54.
32. Griffin TJ, Lock CM, Li XJ, et al. Abundance ratio-dependent proteomic analysis by mass spectrometry. *Anal Chem*. 2003;75:867-874.
33. Zhang CY, Xia RH, Han J, et al. Adenoid cystic carcinoma of the head and neck: clinicopathologic analysis of 218 cases in a Chinese population. *Oral Surg Oral Med Oral Pathol Oral Radiol*. 2013;115:368-375.
34. Ju J, Li Y, Chai J, et al. The role of perineural invasion on head and neck adenoid cystic carcinoma prognosis: a systematic review and meta-analysis. *Oral Surg Oral Med Oral Pathol Oral Radiol*. 2016;122:691-701.
35. van Weert S, van der Waal I, Witte BI, Leemans CR, Bloemena E. Histopathological grading of adenoid cystic carcinoma of the head and neck: analysis of currently used grading systems and proposal for a simplified grading scheme. *Oral Oncol*. 2015;51:71-76.
36. Li JQ, Xu BJ, Shakhtour B, et al. Variability of in situ proteomic profiling and implications for study design in colorectal tumors. *Int J Oncol*. 2007;31:103-111.
37. Johnston HE, Carter MJ, Larrayoz M, et al. Proteomics profiling of CLL versus healthy B-cells identifies putative therapeutic targets and a subtype-independent signature of spliceosome dysregulation. *Mol Cell Proteomics*. 2018;17:776-791.
38. Flores IL, Kawahara R, Miguel MCC, et al. EEF1 D modulates proliferation and epithelial−mesenchymal transition in oral squamous cell carcinoma. *Clin Sci*. 2016;130:785-799.
39. Tao Y, Gross N, Fan X, et al. Identification of novel enriched recurrent chimeric COL7 A1-UCN2 in human laryngeal cancer samples using deep sequencing. *BMC Cancer*. 2018;18:248.
40. Su Z, Kishida S, Tsubota S, et al. Neurocan, an extracellular chondroitin sulfate proteoglycan, stimulates neuroblastoma cells to promote malignant phenotypes. *Oncotarget*. 2017;8:106296-106310.
41. Rooper LM. Challenges in minor salivary gland biopsies: a practical approach to problematic histologic patterns. *Head Neck Pathol*. 2019 Mar 18. https://doi.org/10.1007/s12105-019-01010-8. [Epub ahead of print].

Reprint requests:

Pablo Agustin Vargas
Department of Oral Diagnosis
Piracicaba Dental School
University of Campinas
Av. Limeira, 901 Postal Code: 13414-903
Piracicaba
São Paulo
Brazil.
pavargas@unicamp.br